

# NICKEL NANOPARTICLES CATALYST FOR EFFECTIVE DEGRADATION OF CARMOISINE A IN AQUEOUS ALKALINE MEDIUM BY USING HEXACYANOFERRATE (III) IONS AS A REDUCTANT : A KINETIC STUDY

SHIVANI\* AND ANJALI GOEL

*Department of Chemistry, Kanya Gurukul Campus, Gurukul kangri (Deemed to be University), Haridwar, Uttarakhand, India*

(Received 16 December, 2020; Accepted 21 February, 2021)

## ABSTRACT

The degradation of Carmoisine A, a mono azo dye, by hexacyanoferrate(III) ions in the aqueous alkaline medium using nickel nanoparticles as catalyst has been investigated by kinetic – spectrophotometric method at  $\lambda_{\max}$  515 nm of the reaction mixture. The effect of different parameters like concentration of dye, concentration of oxidant, and pH of the solution on the rate of reaction have been studied under the same experimental conditions. The results show that the degradation rate of the dye increases linearly with the increase in concentrations of oxidant and dye at optimum pH of 7.5 and constant temperature of  $40 \pm 0.1^\circ\text{C}$ . Thermodynamic parameters such as energy of activation ( $E_a$ ), enthalpy of activation ( $\Delta H^\ddagger$ ), entropy of activation ( $\Delta S^\ddagger$ ), frequency factor(A) and free energy of activation ( $\Delta F^\ddagger$ ) have been calculated by studying the reaction rate at four different temperatures, i.e. 40–55°C. UV-Vis, HPLC and LC-MS methods of analysis of degradation products reveals that degraded products are simple and less hazardous.

**KEY WORDS :** Kinetic, Hexacyanoferrate(III) ions, Degradation, Carmoisine A, Mechanism.

## INTRODUCTION

In the textile industry, azo dyes are common synthetic colorants. The wastewater from textile processes, kraft mills, tanneries, foods, cosmetics, and other dyeing processes are strongly colored and contain high concentrations of organic pollutants, which are toxic and carcinogenic to aquatic life (Benkhaya *et al.*, 2017; Bilal *et al.*, 2018; Bilal *et al.*, 2019). One of the extensively used dyes in the textile industries is azo dyes, which are among the most important pollutants in the water. The azo dyes are hardly degraded due to their properties, for example complex molecular structure, high chemical stability and low biodegradability (Chao *et al.*, 2020; Brüsweiler *et al.*, 2017).

The elimination of colour from dye-bearing wastewaters is becoming one of the major environmental problems. Effluent derived from the textile and dyestuff activities can cause serious

environmental impact, not only affecting aesthetic merit but also reducing light penetration and photosynthesis. Furthermore, some are considered toxic and even carcinogenic for human health (Fosso-Kankeu *et al.*, 2018; Tsui *et al.*, 2003; Gong *et al.*, 2009).

Up to now, the removal of azo dyes in wastewater mainly includes physical, chemical, biological methods or combination of various methods, such as electrochemical treatment, ozonation, photocatalysis, Fenton or Fenton-like reagents. Nevertheless, many of these methods are often ineffective for the decomposition of azo dyes and result in large quantities of solid wastes or other environmental problems during the treatment processes (Hameed *et al.*, 2008; Forgacs *et al.*, 2004; Guo *et al.*, 2011; Han *et al.*, 2009; He *et al.*, 2005).

This study is focused on the degradation of Carmoisine A in aqueous alkaline medium by using hexacyanoferrate (abbreviated as HCF) (III) ions

using nickel nanoparticles as a catalyst. The study throws light on kinetics and suitable mechanism of oxidation of azo dye Carmoisine A by alkaline hexacyanoferrate(III) ions on the basis of kinetic and thermodynamic results. HCF(III) ions are commonly used to oxidize numerous organic and inorganic compounds in alkaline medium (Hoch *et al.*, 2008; Sharanabasamma *et al.*, 2011; Zhang *et al.*, 2011). Previously we extended the oxidation capability of HCF(III) ions to the degradation of some azo dyes using mono and bimetallic nanoparticles as Ir, Ir-Cu, Ir-Ni and Ir- Sn as catalyst. These nanoparticles show good catalytic activity and stability (Shimpi *et al.*, 2014; Goel *et al.*, 2016; Goel *et al.*, 2014; Goel *et al.*, 2012) but rare abundance and high cost of Ir restricts its use. Thus, in the present work the authors have discussed the oxidation of Carmoisine A by hexacyanoferrate(III) ions in aqueous alkaline medium using nickel nanoparticles as a catalyst in place of iridium nanoparticles.

## MATERIALS AND METHODS

Azo dye Carmoisine A (chemical structure as shown in Figure 1) was purchased from Loba Chemie (Loba Chemie Pvt. Ltd, Mumbai, India). All reagents used were of analytical grade. The measurements of the pH of the reaction mixture was done on digital pH meter (Systronics  $\mu$ -pH System 361), which was adjusted by using solutions of  $\text{KH}_2\text{PO}_4$  as buffer and NaOH.  $\lambda_{\text{max}}$  of the reaction mixture was measured by using Systronics-117 spectrophotometer in the range 220– 480 nm. The HPLC chromatogram and LC-MS spectra was measured by LC-MS spectrometer model Q-ToF Micro Waters.

### Kinetic - Study

The kinetic experiments were carried out at pH (7.5) and constant temperature ( $40 \pm 0.1$  °C). The required amount of each reactant was thermostated at 40°C to attain thermal equilibrium. The proper quantities of

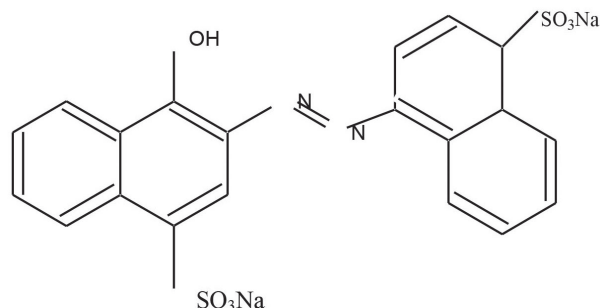


Fig. 1. Chemical structure of Carmoisine A.

reactants were mixed in a 250 ml iodine flask. The reaction was started by taking the solution of Carmoisine A into the prepared reaction mixture of HCF(III) and Ni nanoparticles. The evolution of the reaction was recorded spectrophotometrically with a spectrometric quartz cell at 515nm ( $\lambda_{\text{max}}$ ) of the reaction mixture. It was confirmed that there is neglect interference from other species present in the reaction mixture at this wavelength. As the reaction proceeds, the absorbance of the reaction mixture decreases with time shows a linear affiliation between dye concentration and absorbance. Initial rate ( $dA/dt$ ) of reaction rate was calculated from the slope of concentration vs. time. The first-order rate constant was calculated by the plot of  $\log(a-x)$  versus time with slope equal to  $-k_1/2.303$ . The products were extracted by ethyl acetate using solvent extraction method and identified by LC-MS. Mobile phase for the extracted products of Carmoisine A consisted of methanol: water: acetonitrile (1:2:1).

### Analytical methods

The reaction mixture was kept at atmospheric conditions for 24 hrs and the products were extracted with ethyl acetate. The degradation of dye and identification of degradation products were characterized by UV-Vis spectroscopy (systronic-117), LC-MS (model Q-ToF Micro Waters). The mobile phase consisted of methanol: water: acetonitrile at (1:2:1) at the flow rate of 600  $\mu\text{L}/\text{min}$ .

## RESULTS AND DISCUSSION

The oxidation kinetics of Carmoisine A has been studied at constant pH (7.5) and temperature ( $40 \pm 0.1$ °C) at different concentrations of one reactant keeping the constant concentration of other reactants spectrophotometrically.

### Effect of PVP, CTAB, SDS supported nickel nanoparticles (catalyst)

The nickel nanoparticles were synthesized by modified polyol method by using different surfactants as PVP, CTAB, SDS with ethylene glycol (EG) as solvent as reported earlier for Ir nanoparticles synthesis (Chaudhary *et al.*, 2017) Further the effect of these nanoparticles as catalyst on the reaction rate has been studied. In figure 2 the data reveals that PVP supported nickel nanoparticles show the maximum reaction rate as compared to other surfactant assisted nanoparticles.

Thus study has been made with PVP supported Ni-nanoparticles as catalyst.

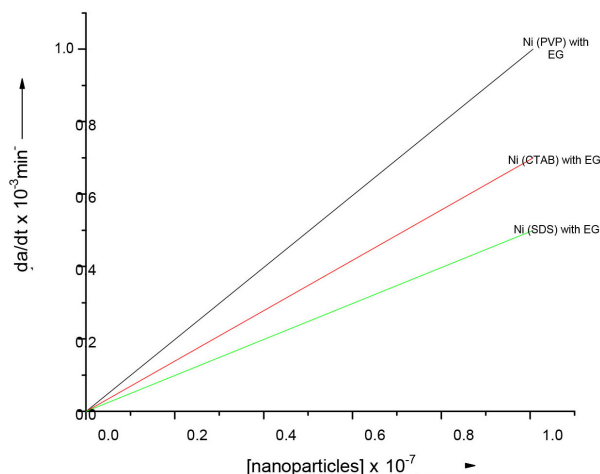


**Fig. 2.** Effect of different nanoparticles on the rate of degradation of Carmoisine A. Experimental conditions pH = 7.5; [HCF(III)] =  $3 \times 10^{-6}$  mol/dm<sup>3</sup>; [catalyst] =  $1.006 \times 10^{-7}$  mol/dm<sup>3</sup>; temperature =  $40 \pm 0.1^\circ\text{C}$ .

Figure 6 show a gradual increase in the reaction rate with the increase of catalyst concentration. These results reveal that reaction follows first order kinetics with respect to catalyst concentration. The nickel PVP supported Ni nanoparticles show good catalytic activity as compare to nickel precursor.

**Effect of pH**

The pH of the reaction mixture plays an important role in the degradation of organic compounds. In the case of ionic reactions, the pH affects ionization and the optimum value is required at which ionization is maximum and then the rate of reaction is measured at that pH value. The effect of pH on the degradation of Carmoisine A was studied by varying pH of solution from 6 to 7.5. As the colour of Carmoisine A becomes dark above 7.5, the higher range of pH has not been considered for the oxidation dye. Figure 3 shows that the pH for the degradation of Carmoisine A is 7.5 representing the maximum ionization in this range. It was not found possible to study reaction in the acidic pH range, that is, below 7 due to the electrostatic interaction between hydrogen ion and dye molecule.

**Effect of HCF(III)**

To study the effect of oxidant concentration of HCF(III) ions on the degradation rate of Carmoisine A, concentration of HCF(III) ions was varied from  $1 \times 10^{-6}$  to  $9 \times 10^{-6}$  mol/dm<sup>3</sup>. Figure 4 shows that with

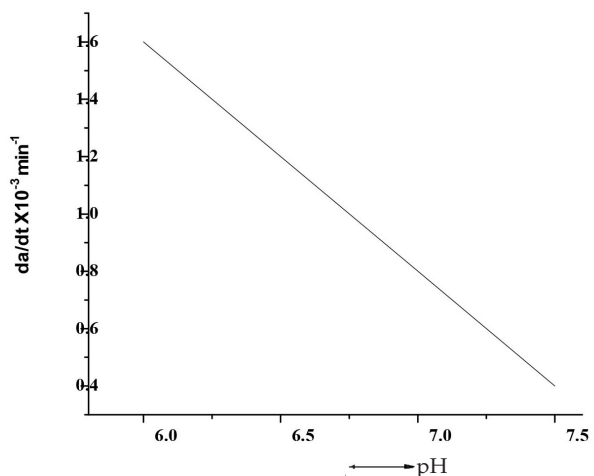


**Fig. 3.** Effect of pH on the degradation rate of Carmoisine A. Experimental conditions [Carmoisine A] =  $3 \times 10^{-5}$  mol/dm<sup>3</sup>; [HCF(III)] =  $3 \times 10^{-6}$  mol/dm<sup>3</sup>; [Catalyst] =  $1.006 \times 10^{-7}$  mol/dm<sup>3</sup> temperature =  $40 \pm 0.1^\circ\text{C}$ .

the increase in oxidant concentration, the rate of degradation of Carmoisine A increases. A straight line between the concentration of HCF(III) and rate of reaction indicates that reactions follows first order kinetics with respect to [HCF(III)].

**Effect of substrate**

The effect of variation of substrate concentration ( $1 \times 10^{-5}$  to  $9 \times 10^{-5}$  mol/dm<sup>3</sup>) on reaction rate was studied. On increasing the dye concentration rate of degradation increases linearly because more molecules of dyes are available for degradation.

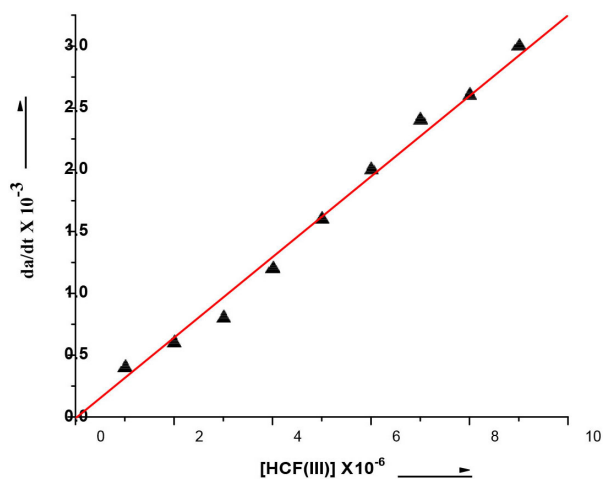


**Fig. 4.** Effect of [HCF(III)] ions on the degradation rate of Carmoisine A. Experimental conditions [Carmoisine A] =  $3 \times 10^{-5}$  mol/dm<sup>3</sup>; [catalyst]=  $1.006 \times 10^{-7}$  mol/dm<sup>3</sup>; pH = 7.5; temperature =  $40 \pm 0.1^\circ\text{C}$ .

Data presented as Figure 5 shows that reaction follows first-order kinetics with respect to dye concentration.

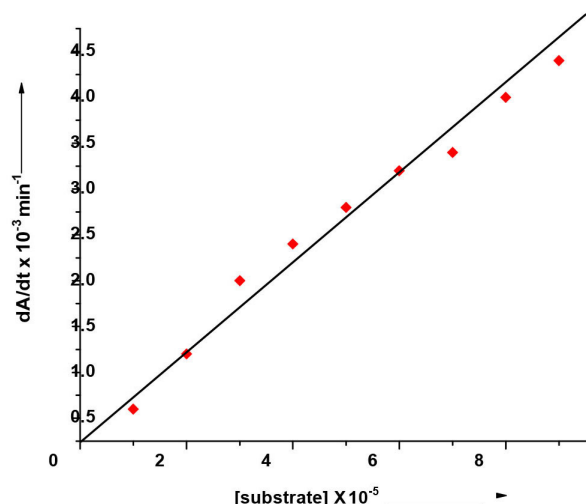


Fig. 5. Effect of [Carmoisine A] ions on the degradation rate of Carmoisine A. Experimental conditions [HCF(III)] =  $3 \times 10^{-6}$  mol/dm<sup>3</sup>; [catalyst] =  $1.006 \times 10^{-7}$  mol/dm<sup>3</sup>; pH = 7.5; temperature =  $40 \pm 0.1^\circ\text{C}$ .

### Effect of temperature

Thermodynamic parameters including activation energy ( $E_a$ ), pre-exponential factor ( $A$ ), enthalpy of activation ( $\Delta H^\ddagger$ ), entropy of activation ( $\Delta S^\ddagger$ ) and free energy of activation ( $\Delta F^\ddagger$ ) for the oxidation of Carmoisine A by HCF(III) ions have been calculated by studying the reaction at four different temperatures ( $T$ ), that i.e. 40, 45, 50, and  $55^\circ\text{C}$ . In

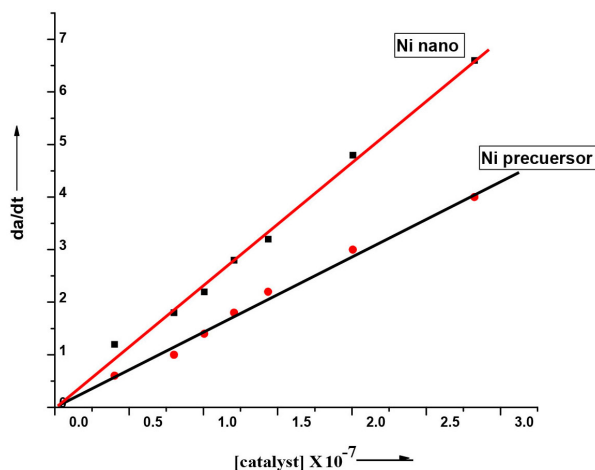


Fig. 6. Effect of [catalyst] and [precursor] on the rate of degradation of Carmoisine A. Experimental conditions pH = 7.5; [HCF(III)] =  $3 \times 10^{-6}$  mol/dm<sup>3</sup>; [Carmoisine A] =  $3 \times 10^{-5}$  mol/dm<sup>3</sup>; temperature =  $40 \pm 0.1^\circ\text{C}$ .

Figure 7 Arrhenius plot shows a linear relationship between temperature and reaction rate. High value of pre-exponential factor signifies large size of reacting species (Table 1). Further, the reaction was characterized by a more negative value of entropy of activation reveals the formation of polar species and a low value of activation energy show good catalytic activity of nickel nanoparticles.

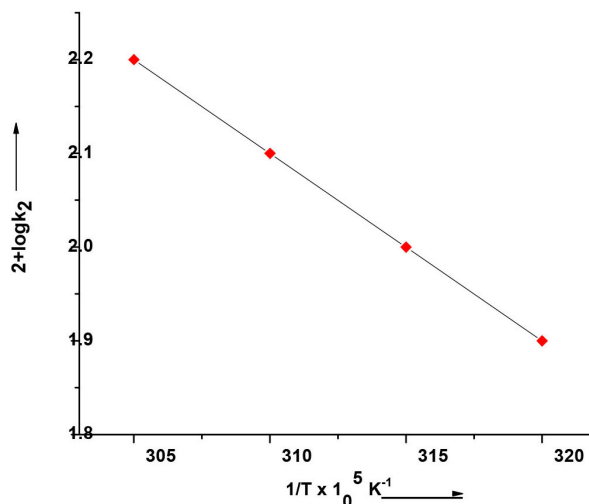


Fig. 7. Arrhenius plot for initial degradation of MY by [HCF(III)] ions. Experimental condition [Carmoisine A] =  $5 \times 10^{-5}$  mol/dm<sup>3</sup>; [HCF(III)] =  $5 \times 10^{-6}$  mol/dm<sup>3</sup>; [catalyst] =  $1.006 \times 10^{-7}$  mol/dm<sup>3</sup>; temperature =  $40 \pm 0.1^\circ\text{C}$  to  $55 \pm 1^\circ\text{C}$ .

Table 1. Values of thermodynamic parameters

S. No.	Thermodynamic parameters	Values [Carmoisine A]
1	$E_a$ (kJ/mol)	24.64
2	$A$ ( $\text{l mol}^{-1} \text{sec}^{-1}$ )	$1.121 \times 10^4$
3	$\Delta S^\ddagger$ (e.u.)	-40.87
4	$\Delta H^\ddagger$ (kJ/mol)	21.97
5	$\Delta F^\ddagger$ (kJ/mol)	76.8

### Identification of degradation products of Carmoisine A UV-Vis Spectroscopy

UV-Vis spectroscopy is used as a primary technique to determine the degradation of dye. Degradation of Carmoisine A was monitored by UV-Vis spectrophotometer (systronic 117). Figure 8 shows that Carmoisine A has maximum absorption at 515nm (Lasyal *et al.*, 2016) which after degradation disappears and a new peak forms at 257nm. Formation of new peak verifies the degradation of dye into some new substance/substances.

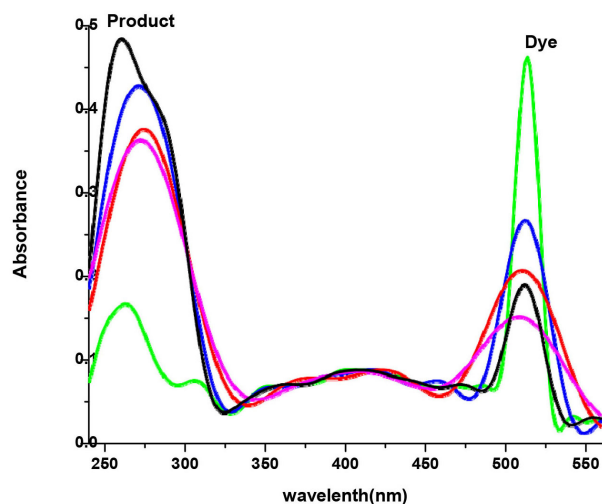


Fig. 8. UV-Vis spectra of Carmoisine A before and after degradation.

LCMS

Liquid chromatography–mass spectrometry (LC-MS) is an analytical technique that combines the physical separation capabilities of liquid chromatography (HPLC) with the mass analysis capabilities of mass spectrometry (MS). Hence in the present study LC-MS has been used to confirm degradation of dye and to investigate the products formed by the degradation. In Figure 9 HPLC chromatogram show two major peaks at retention time 2.72 and 3.23 min<sup>-1</sup>. LCMS spectra (Fig. 10) also show two major peaks along with some small peaks indicating the formation of two major products along with some minor products by the degradation of Carmoisine A dye.

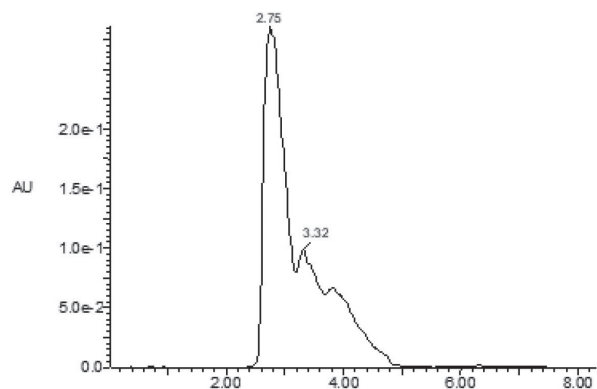


Fig. 9. HPLC chromatogram of degradation products.

Thus the formation of two major products occurs by the breakage of azo linkage as 3-naphthol-4-hydroxy naphthalene sulphonic acid and 3-amino-4-hydroxy naphthalene sodium sulphate. These two

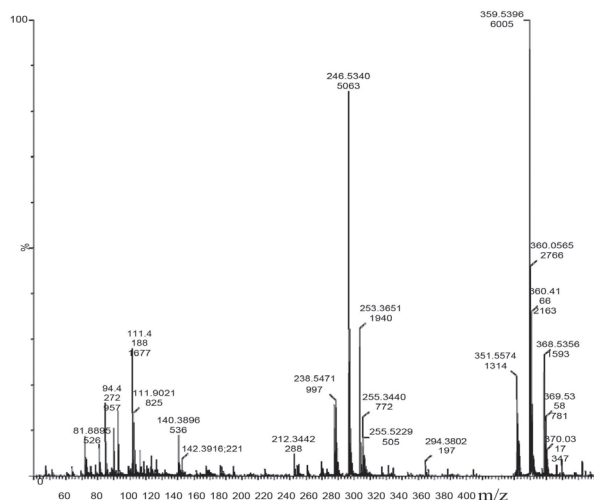


Fig. 10. LC-MS spectra of degradation products of Carmoisine A.

major products further oxidized to give simple and less hazardous compounds like propanoic acid, toluene, 4- phenyl butanoic acid, 3- phenyl propanaldehyde, 1,4- naphthoquinone, 1- hydroxy

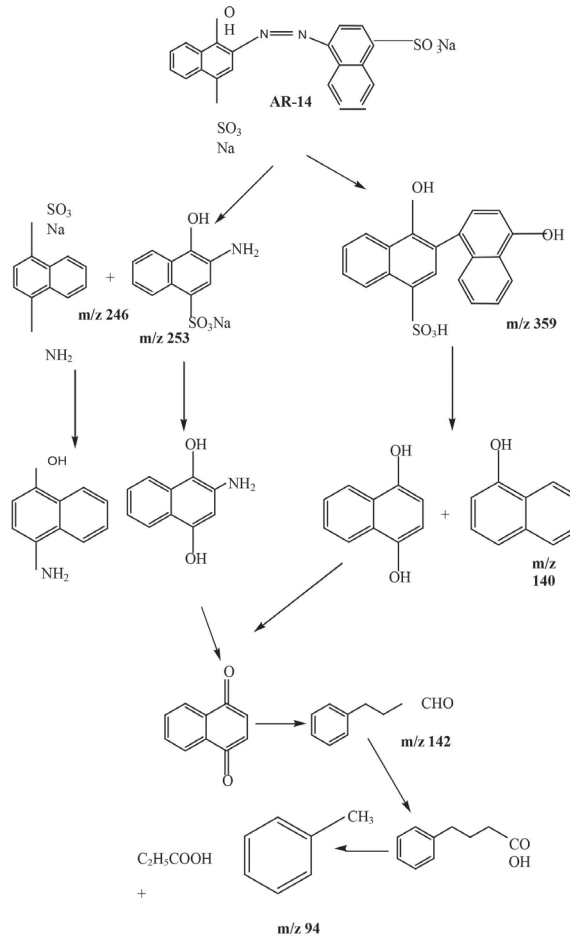
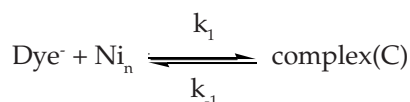


Fig. 11. Proposed mechanism for the degradation of Carmoisine A.

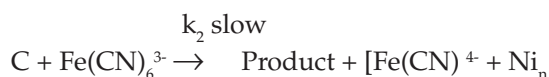
naphthalene, 1,4- di hydroxy naphthalene, 1-hydroxy- 4-amino naphthalene, 1,4- di hydroxy -3-amino naphthalene, , 4-amino naphthalene sodium sulphate.

### Mechanism

Based on the above kinetic study, thermodynamic data, product analysis, and previously reported work (Goel *et al.*, 2019) the following reaction mechanism for the oxidation of Carmoisine A has been proposed. According to the mechanism, it is assumed that dye molecule exists as an anion in the aqueous alkaline medium which forms a weakly bonded complex (C). This complex dissociates with HCF(III) ions through a slow step into product along with  $Ni_n$ .



### Derived rate law



Based on the above mechanism and experimental facts, the following rate law has been derived.

$$r = k_2 \cdot k_1 / k_{-1} [\text{Dye}][\text{HCF(III)}][Ni_n]$$

which is similar to the following experimental rate law

$$R_{obs} = k_2 [\text{Dye}][\text{HCF(III)}][Ni_n] \\ \text{where } k = k_1/k_{-1}.$$

### CONCLUSION

The kinetic–spectrophotometric study of the oxidation of Carmoisine A by hexacyanoferrate(III) ions in aqueous alkaline medium proves HCF(III) is a good oxidant for degradation of dye. Kinetic study of Carmoisine A by HCF(III) ions follows first-order reaction rate with respect to the substrate and HCF(III) concentrations at pH 7.5 and at constant temperature of  $40 \pm 0.1$  °C. A suitable mechanism for the degradation of Carmoisine A has been proposed. Product analysis shows that the degradation of dye Carmoisine A results in the formation of less hazardous products. The comparison of the catalytic activity of nickel nanoparticles with the reported iridium nanoparticles (Goel *et al.*, 2018) under the same experimental conditions, it can be concluded though the requirement of nickel

nanoparticles is approx three times more than that of iridium nanoparticles to get the same degradation rates but about thousands time low cost of nickel metal than iridium metal makes the present method superior and beneficial for commercial use of dye degradation.

### REFERENCES

- Benkhaya, S., El Harfi, S. and El Harfi, A. 2017. Classifications, properties and applications of textile dyes: A review. *Appl. J. Environ. Eng. Sci.* 3(3): 00000-3.
- Bilal, M., Rasheed, T., Iqbal, H.M., Li, C., Wang, H., Hu, H., Wang, W. and Zhang, X. 2018. Photocatalytic degradation, toxicological assessment and degradation pathway of CI Reactive Blue 19 dye. *Chem Eng Res Des.* 129 : 384-390.
- Bilal, M., Rasheed, T., Nabeel, F., Iqbal, H.M. and Zhao, Y. 2019. Hazardous contaminants in the environment and their laccase-assisted degradation-a review. *J. Environ. Manage.* 234 : 253-264.
- Brüschweiler, B.J. and Merlot, C. 2017. Azo dyes in clothing textiles can be cleaved into a series of mutagenic aromatic amines which are not regulated yet. *Regul. Toxicol. Pharmacol.* 88 : 214-226.
- Chao, H.J., Xue, D., Jiang, W., Li, D., Hu, Z., Kang, J. and Liu, D. 2020. A lowvoltage pulse electrolysis method for the degradation of anthraquinone and azo dyes in chloride medium by anodic oxidation on Ti/IrO<sub>2</sub>RuO<sub>2</sub>SnO<sub>2</sub> electrodes. *Water Environ. Res.* 92(5) : 779-788.
- Forgacs, E., Cserhati, T. and Oros, G. 2004. Removal of synthetic dyes from wastewaters: a review. *Environ Int.* 30 (7) : 953-971.
- Gong, J.L., Wang, B., Zeng, G.M., Yang, C.P., Niu, C.G., Niu, Q.Y., Zhou, W.J. and Liang, Y. 2009. Removal of cationic dyes from aqueous solution using magnetic multi-wall carbon nanotube nanocomposite as adsorbent. *J. Hazard. Mater.* 164 (2-3) : 1517-1522.
- Goel, A. and Lasyal, R. 2016. Degradation of Orange G dye by hexacyanoferrate (III) ions in the presence of Iridium nanoparticles: effect of system parameters and kinetic study. *Desalin. Water Treat.* 57 (37) : 17547-17556.
- Goel, A. and Chaudhary, M. 2018. Highly dispersed PVP-supported Ir-Ni bimetallic nanoparticles as high performance catalyst for degradation of metanil yellow. *Bull. Mater. Sci.* 41 (3) : 81.
- Goel, A. and Abhilasha. 2016. A kinetic and mechanistic study on degradation of acid orange -IV using HCF(III) ions in aqueous alkaline medium. *International Journal of Theoretical and Applied Sciences.* 8 (2) : 76-81.
- Goel, A., Bhatt, R. and Lasyal, R. 2014. Kinetic and

- mechanistic study of the oxidation of orange II by hexacyanoferrate(III) ions catalyzed by iridium nanoclusters. *Int. J. Chem. Sci.* 12 (4) : 1527-1537.
- Goel, A., Bhatt, R. and Rani, N. 2012. Removal of methyl orange, an azo dye, using oxidative degradation by hexacyanoferrate (III) ions. *Discovery Science.* 2:4.
- Goel, A. and Chaudhary, M. 2019. A novel method for oxidative degradation of metanil yellow azo dye by hexacyanoferrate (III) ions. *Water Environ. Res.* 91 (1) : 69-74.
- Goel, A. and Lasyal, R. 2018. Facile synthesis of IrO<sub>2</sub> nanoclusters and their application as catalyst in the degradation of azo dyes. *Turk. J. Chem.* 42 : 941-957.
- Guo, J., Jiang, D., Wu, Y., Zhou, P. and Lan, Y. 2011. Degradation of methyl orange by Zn (0) assisted with silica gel. *J. Hazard. Mater.* 194 : 290-296.
- Hameed, B.H. and El-Khaiary, M.I. 2008. Equilibrium, kinetics and mechanism of malachite green adsorption on activated carbon prepared from bamboo by K<sub>2</sub>CO<sub>3</sub> activation and subsequent gasification with CO<sub>2</sub>. *J. Hazard. Mater.* 157 (2-3) : 344-351.
- Han, F., Kambala, V.S.R., Srinivasan, M., Rajarathnam, D. and Naidu, R. 2009. Tailored titanium dioxide photocatalysts for the degradation of organic dyes in wastewater treatment: a review. *Appl Catal A Gen.* 359 (1-2) : 25-40.
- He, F. and Zhao, D. 2005. Preparation and characterization of a new class of starch-stabilized bimetallic nanoparticles for degradation of chlorinated hydrocarbons in water. *Environ. Sci. Technol.* 39 (9) : 3314-3320.
- Hoch, L.B., Mack, E.J., Hydutsky, B.W., Hershman, J.M., Skluzacek, J.M. and Mallouk, T.E. 2008. Carbothermal synthesis of carbon-supported nanoscale zero-valent iron particles for the remediation of hexavalent chromium. *Environ. Sci. Technol.* 42 (7) : 2600-2605.
- Lasyal, R. and Goel, A. 2016. Degradation of Azo Dye, Acid Red-14 by Hexacyanoferrate (III) Using Iridium Nanoclusters: A Kinetic Study. *Asian J. Chem.* 28 (2) : 335.
- Mbu, E.E., Ntwampe, S.K., Nyembwe, K.J., Fosso-Kankeu, E. and Dodoo-Arhin, D. 2018. Photocatalytic degradation of azo and rhodamine dyes using copper (ii) oxide nanoparticles. <https://doi.org/10.17758/EARES4.EAP1118210>
- Sharanabasamma, K., Angadi, M.A. and Tuwar, S.M. 2011. Kinetics and mechanism of ruthenium (III) catalyzed oxidation of L-proline by hexacyanoferrate (III) in aqueous alkali. *The Open Catalysis Journal* 4: 1-8.
- Shimpi, R., Fadat, R., Janrao, D.M. and Farooqui, M. 2014. A kinetic and mechanistic study on the oxidation of sulfanilamide by hexacyanoferrate (III) in aqueous alkaline medium. *J. Chem. Pharm. Res.* 6(6) : 1011-1019.
- Tsui, L.S., Roy, W.R. and Cole, M.A. 2003. Removal of dissolved textile dyes from wastewater by a compost sorbent. *Color. Technol.* 119(1) : 14-18.
- Zhang, Y.J., Liu, G.R., Li, D.P., Tian, Y.X., Zhang, L. and Li, L. 2011. Solid Super Acid of S<sub>2</sub>O<sub>8</sub><sup>2-</sup>/Fe<sub>x</sub>O<sub>y</sub>-CuO<sub>x</sub> Catalytic Degradation of Orange IV. *Adv Mat Res* 239 : 182-185. Trans Tech Publications Ltd.
-